Nonmigrating tidal signals in the thermospheric zonal wind as seen by CHAMP and TIME-GCM

K. Häusler,[1] H. Lühr,[1] M. E. Hagan,[2] A. Maute[2] and R. G. Roble[2]

K. Häusler, H. Lühr, Helmholtz Centre Potsdam, GFZ German Research Centre for Geosciences, Telegrafenberg, 14473 Potsdam, Germany. (kathrin@gfz-potsdam.de)

M. E. Hagan, A. Maute, and R. G. Roble, High Altitude Observatory, National Center for Atmospheric Research, Boulder, CO 80307, USA.

[1]Helmholtz Centre Potsdam, GFZ German Research Centre for Geosciences, Potsdam, Germany.

[2]High Altitude Observatory, National Center for Atmospheric Research, Boulder, Colorado, USA.

Abstract.

Four years (2002-2005) of continuous accelerometer measurements taken onboard the CHAMP satellite (orbit altitude ∼400 km) present a unique opportunity to investigate the thermospheric zonal wind on a global scale. Recently we were able to relate the identified wave-4 structure in the zonal wind at equatorial latitudes to the influence of nonmigrating tides and in particular to the eastward propagating diurnal tide with zonal wavenumber 3 (DE3). The DE3 tide is primarily excited by latent heat release in the tropical troposphere in deep convective clouds and thus was not expected to be found at 400 km altitude. In order to investigate the mechanisms that couple the tidal signals all the way to the upper thermosphere we started a comparison with the thermosphere-ionosphere-mesosphere-electrodynamics general circulation model (TIME-GCM) developed at the National Center for Atmospheric Research (NCAR). Therefore, the model output was processed the same way as the satellite data. Initial results show good agreement between the model and the satellite data for the June simulations especially for DE3. Yet the model is underestimating the eastward propagating zonal wavenumber 2 diurnal tide (DE2) which is quite prominent in the CHAMP data. Furthermore, the model predicts for most tidal components increasing amplitudes with an increasing solar flux level. However, a stronger solar flux level is diminishing the prominent DE3. We can confirm the dependence on the solar flux level for the nonmigrating tidal signatures in CHAMP data for most components as well.

1. Introduction

Numerous satellite missions like e.g. TIMED (Thermosphere Ionosphere Mesosphere Energetics and Dynamics), ROCSAT-1 (Republic of China Satellite 1), and CHAMP (CHAllenging Minisatellite Payload) provide innovative continuous and globally distributed measurements of the parameters of the upper atmosphere. Thereby, growing evidence is presented that upward propagating tides from as low as the troposphere are able to modulate upper atmospheric quantities. Häusler et al. [2007] report on a dominating wave-4 structure seen in the CHAMP zonal wind at 400 km altitude during certain local times (LT). In a recent study, Häusler and Lühr [2009, submitted] were able to relate the identified wave-4 pattern in the zonal wind to the presence of the eastward propagating diurnal tide with zonal wavenumber 3 (DE3) which is evident as a wave-4 structure when observed from Sun-synchronous orbits. The origin of DE3 is the tropical troposphere where it is excited by latent heat release in deep convective clouds. Performing numerical experiments with the thermosphere-ionosphere-mesosphere-electrodynamics general circulation model (TIME-GCM), *Hagan et al.* [2007] explored the effects of tides with tropospheric sources on the upper and middle atmosphere and demonstrated thereby that DE3 is capable of penetrating from the troposphere to the thermosphere. Furthermore, the nonlinear interaction between the DE3 and the migrating diurnal tide (DW1) generates a stationary planetary wave-4 oscillation (sPW4) in the mesosphere and lower thermosphere (MLT) region which may impact the E region dynamo as well as the atmospheric dynamics aloft [*Hagan et al.*, 2009].

In this report, we want to explore in situ measurements from CHAMP and TIME-GCM simulations in order to quantify the performance of the TIME-GCM model concerning tidal signatures in the upper thermosphere. Eventually, we want to use the model to perform numerical experiments identifying the coupling mechanisms between the various atmospheric layers.

2. Model and data analysis

The TIME-GCM is a three dimensional time-dependent global grid point model that calculates the dynamics, electrodynamics, photoionization, neutral gas heating, and the compositional structure of the middle and upper atmosphere. A more complete description of the model, which was developed at the National Center for Atmospheric Research, is given by Roble [1995, 1996] and Roble and Ridley [1994] and references therein. TIME-GCM is able to provide inherently the atmospheric tides that are excited by the absorption of ultraviolet and extreme ultraviolet radiation in the middle and upper atmosphere. Nevertheless, it cannot account for tidal components that are excited by latent heat release in deep tropical clouds or by the absorption of infrared radiation [*Hagan et al.*, 2007]. In order to get the tides of tropospheric origin into the TIME-GCM, the lower boundary (i.e., 10 mb; $\sim$30 km) of the model is disturbed with results of the global scale wave model (GSWM) which can account for the missing tides [e.g., *Hagan and Forbes*, 2002, 2003].

For the simulations discussed herein, we ran the TIME-GCM with 2.5° by 2.5° horizontal resolution and 4 grid points per scale height in the vertical. For the March, June, September, and December simulations, the 10.7-cm solar radio flux (F10.7) value was set to 75, the hemispheric power value [after *Evans*, 1987] to 8 GW, and the cross-cap potential drop to 30 kV. The June simulations were also run for F10.7 = 120 and F10.7 = 200.

The CHAMP data set used for the comparison with TIME-GCM is the same as described in Häusler and Lühr [2009, submitted]. Four years of CHAMP zonal wind measurements taken between 2002-2005 have been analyzed for nonmigrating tidal signatures for each month of the year. The processing steps are briefly described as follows. First, a daily zonal mean consisting of 15 consecutive orbits centered around the orbit of interest is removed from an overflight averaged within a select latitude band. There are about 42,500 overflights available and the obtained zonal wind residuals are then binned into months, LT intervals, and 24 longitude bins. Performing a 2D-FFT on the data yields the desired tidal spectra. For further information on the data processing see Häusler and Lühr [2009, submitted].

In order to get a reasonable comparison, the TIME-GCM output was processed in the same way as the CHAMP data after calculating the LT following each of the aforementioned steps. Due to the model resolution, the latitude band around the equator ranges from 11.25°N - 11.25°S for TIME-GCM compared to 10°N - 10°S for CHAMP. The examined altitude is about 400 km.

3. Results

We started our simulations with an F10.7 value of 75 and let the model run to get a diurnally reproduceable state for March, June, September, and December. The GSWM lower boundary forcing included westward propagating zonal wavenumber 6 (W6) through eastward propagating zonal wavenumber 6 (E6) diurnal and semidiurnal components. Figure 1 displays the tidal spectra of the zonal wind for TIME-GCM and CHAMP for the diurnal (D) westward (W) propagating tides from zonal wavenumber 7 (DW7) to the diurnal eastward (E) propagating tides with zonal wavenumber 5 (DE5), the semidiurnal

(S) tides from SW8 to SE4, as well as the stationary planetary waves from sPW1 to sPW6 at the equator. Due to the slow precession of CHAMP through LT we have to keep in mind that the calculated tides for each month are composites of four years. The corresponding mean F10.7 value for the month of March is 128, for June 120, for September 122, and for December 118.

Focusing first on the prominent DE3 it is clear to see that it is dominating the diurnal tidal spectrum of TIME-GCM. The biggest amplitude of 13.9 m/s is obtained in September. March and December reach amplitudes of 10.8 m/s and 10.7 m/s, respectively, and for June an amplitude of 5.8 m/s is calculated. The corresponding amplitudes of DE3 for CHAMP are much smaller and display different seasonal variability. DE3 amplitudes equal 3.2 m/s for March, 3.1 m/s for June, 6.2 m/s for September, and 2.0 m/s for December. Häusler and Lühr [2009, submitted] report that DE3 has a pronounced maximum from July to October peaking in July with an amplitude of 6.7 m/s and a smaller maximum in the month of March/April (3.6 m/s).

Notably during March, June, and December, the SE2 is dominating the TIME-GCM semidiurnal spectrum with amplitudes ranging from 3.3 m/s to 4.7 m/s. This behavior can be attributed to the strong DE3 and the discovered nonlinear interaction between DE3 and DW1 yielding in the generation of SE2 and sPW4 [*Hagan et al.*, 2009]. In the CHAMP tidal analysis, SE2 is also present but with reduced amplitudes ranging from 1.0 m/s to 1.6 m/s. The model SE2 and the CHAMP SE2 exhibit very different behavior during the course of the year.

The diurnal tide dominating the CHAMP tidal spectrum for the month of June is DE2 with an amplitude of 7.7 m/s. During December this tidal mode reaches 5.7 m/s and in

March and September 3.3 m/s and 2.9 m/s, respectively. Only in December DE2 can be found in the TIME-GCM tidal analysis with an amplitude of 8.0 m/s whereas for all the other months the amplitudes are below 1.5 m/s.

Due to the fact that the June model run resulted in a reasonable amplitude for DE3 and the westward propagating tides are in good agreement with CHAMP observations we decided to focus on June simulations for the investigation of a possible solar flux dependence. Therefore, TIME-GCM was run again for June for a F10.7 value of 120 and 200 keeping all the other parameters described earlier constant. Figure 2 shows the results for the model simulations for different solar flux conditions. Displayed as well are the CHAMP results already presented in Figure 1. In general one can say that for most components the model predicts increasing amplitudes with an increasing solar flux level. Though for DE3 and SE4 a clear decrease in amplitudes are predicted for an increase in solar flux level. For DE3 that means in detail that its amplitude decreased from 5.7 m/s for F10.7 = 75 to 4.0 m/s for F10.7 = 120 to 1.5 m/s for F10.7 = 200.

However, to investigate a solar flux dependence of the CHAMP tides, the data have to be processed a little differently. CHAMP is precessing through 24 hour LT within 131 days taking about 11 days for 1 hour LT. Therefore, the described procedure to obtain the tidal signatures out of CHAMP data was applied to a 131 days time window starting from day of year (doy) 1 of 2002. The 131 days time window is then moved through time for every 11 days resulting in 122 individual running data sets for the available 4 years of measurements. The results for DW2, D0, DE2, and DE3 of TIME-GCM and CHAMP are displayed in Figure 3 for the three different solar flux levels. The corresponding time period for the CHAMP data is the 131 days time window centered around doy 177 for 2002, doy 175 for 2003, and doy 170 for 2005. Within the considered time windows mentioned before the solar flux level decreases from F10.7=175 in 2002, to F10.7=128 in 2003, and to F10.7=95 in 2005. Besides the solar flux dependence, Figure 3 also contains information about the latitudinal behavior of the reported tides. Thereby, the latitude range for TIME-GCM is 11.25°-31.25° and 31.25°-51.25° in the northern and southern hemisphere, respectively, and the already discussed ±11.25° around the equator. The latitude band for CHAMP is 10°-30° and 30°-50° in the northern and southern hemisphere, respectively, and ±10° around the equator.

Looking at the latitudinal characteristics of DE3 in Figure 3 it is striking how well the amplitudes of TIME-GCM and CHAMP are matching each other especially at the equator and in the southern hemisphere. Moreover, the CHAMP DE3 reveals the same solar flux dependence as predicted by TIME-GCM. From 2002 to 2005 the amplitudes of DE3 are increasing from 2.2 m/s to 5.0 m/s at the equator where also the maximum of DE3 can be found. DE2 as well is increasing with decreasing solar flux level revealing an amplitude of 2.3 m/s in 2002 compared to 5.4 m/s in 2005. The latitudinal behavior of DE2 and DE3 is similar with bigger amplitudes for DE2. As already mentioned before, TIME-GCM doesn't resolve the DE2 very well. The amplitudes are mostly under 2 m/s and contrary to CHAMP suggesting an increase with increasing solar flux. The observed D0 tidal mode is more prominent in the southern hemisphere peaking at 40°S. Both TIME-GCM and CHAMP largely demonstrate this for for low and middle solar activity. For high solar activity, CHAMP D0 amplitudes are much higher in the northern hemisphere and much lower at the equator and 20°S compared to TIME-GCM. As already mentioned the peak of this tidal mode can be found for both at 40°S revealing an amplitude increase with increasing solar flux level. The DW2 CHAMP and TIME-GCM comparison is not very satisfying. Yet, when looking at the evolution of the CHAMP DW2 over the course of the 4 years, an increase with increasing solar flux is found as well as shown in Figure 2 for the TIME-GCM simulations.

4. Discussion and Summary

We present for the first time a direct comparison of tidal signals in the zonal wind observed in situ by CHAMP and obtained from TIME-GCM simulations. Special emphasis is put on the important DE3 nonmigrating tide which has strong effects on the neutral part of the upper atmosphere as demonstrated by *Oberheide et al.* [2009, submitted]. It was shown in Figure 1 that TIME-GCM is overestimating the strength of DE3 in 400 km altitude in all months except for June. Notably, the biggest difference (8.2 m/s) between the model simulations and in situ measurements is given for the month of December when CHAMP is observing the smallest amplitudes within this month suggesting that TIME-GCM isn't yet capable of reproducing the observed inter-annual variability. Comparing the inter-annual DE3 variability of the CHAMP zonal wind with the MLT zonal wind as reported by Pedatella et al. [2008] it is evident that the observed variability is reliable. Fortunately, the agreement between TIME-GCM and CHAMP for the month of June is remarkably good. Even the predicted solar cycle dependence of DE3 can be confirmed with the CHAMP data.

However, TIME-GCM doesn't predict DE2 which is quite prominent in the CHAMP data and actually exceeding DE3 in June. But GSWM DE2 amplitudes reported by *Hagan and Forbes* [2002] are also comparatively weak suggesting that the observed DE2 discrepancies are actually attributable to a weakness in the GSWM lower boundary condition forcing. According to theory, the nonlinear interaction of DE2 and DW1 would yield the generation of SE1 and sPW3 similar to the reported SE2 and sPW4 for DE3 and DW1 by *Hagan et al.* [2009]. In fact, we observe with CHAMP a strong SE1 with an amplitude of 5.5 m/s when DE2 reaches its maximum in June and the sPW3 is displaying an amplitude of 4.3 m/s (Figure 1). Due to the fact that TIME-GCM isn't resolving DE2 right now a possible connection between DE2 and SE1 and sPW3 cannot be confirmed yet.

Nevertheless, the comparison between TIME-GCM and CHAMP unfolded that the perturbation of the lower boundary of TIME-GCM with the GSWM isn't quite optimal right now yielding in the observed discrepancies. However, both data sets provide evidence for a dependence of the tides on solar flux. Namely, for most components an increasing solar flux level is heading to increasing amplitudes for the westward propagating tides and decreasing amplitudes for the eastward propagating tides.

Acknowledgments. KH is supported by the DFG through its priority program CAWSES (SPP1176), Grants LU446/9-1, LU446/10-1 and the Graduate Student Visitor Program of the Advanced Study Program of the National Center for Atmospheric Research. The National Center for Atmospheric Research is sponsored by the National Science Foundation.

References

Evans, D. S. (1987), Global statistical patterns of auroral phenomena, in *Proceedings of the Symposium on Quantitative Modeling of Magnetospheric-Ionospheric Coupling Processes*, edited by Y. Kamide and R. A. Wolf, pp. 325-330, Kyoto Sangyo Univ., Kyoto, Japan.

Hagan, M. E., and J. M. Forbes (2002), Migrating and nonmigrating diurnal tides in the middle and upper atmosphere excited by tropospheric latent heat release, *J. Geophys. Res.*, *107*(D24), 4754, doi:10.1029/2001JD001236.

Hagan, M. E., and J. M. Forbes (2003), Migrating and nonmigrating semidiurnal tides in the upper atmosphere excited by tropospheric latent heat release, *J. Geophys. Res.*, *108*(A2), 1062, doi:10.1029/2002JA009466.

Hagan, M. E., A. Maute, R. G. Roble, A. D. Richmond, T. J. Immel, and S. L. England (2007), Connections between deep tropical clouds and the Earth's ionosphere, *Geophys. Res. Lett.*, *34*, L20109, doi:10.1029/2007GL030142.

Hagan, M. E., A. Maute, and R. G. Roble (2009), Tropospheric tidal effects on the middle and upper atmosphere, *J. Geophys. Res.*, *114*, A01302, doi:10.1029/2008JA013637.

Häusler, K. and H. Lühr (2009), Nonmigrating tidal signals in the thermospheric zonal wind at dip equator latitudes as observed by CHAMP, *Ann. Geophys.*, submitted..

Häusler, K., H. Lühr, S. Rentz, and W. Köhler (2007), A statistical analysis of longitudinal dependences of upper thermospheric zonal winds at dip equator latitudes derived from CHAMP, *J. Atmos. Solar-Terr. Phys. 69*, 1419-1430, doi:10.1016/j.jastp.2007.04.004.

Oberheide, J., J. M. Forbes, K. Häusler, and Q. Wu (2009), Tropospheric tides from 80-400 km: propagation, inter-annual variability and solar cycle effects, *J. Geophys. Res.*, submitted.

Pedatella, N. M., J. M. Forbes, J. Oberheide (2008), Intra-annual variability of the low-latitude ionosphere due to nonmigrating tides, *Geophys. Res. Lett., 35*, L18104, doi:10.1029/2008GL035332.

Roble, R. G. (1996), The NCAR thermosphere-ionosphere-mesosphere-electrodynamics general circulation model (TIME-GCM), in *STEP Handbook on Ionospheric Models*, edited by R. W. Schunk, pp. 281-288, Utah State University, Logan.

Roble, R. G. (1995), Energetics of the mesosphere and thermosphere, in *The Upper Mesosphere and Lower Thermosphere: A Review of Experiment and Theory, Geophys. Monogr. Ser.*, 87, edited by R. M. Johnson and T. L. Killeen, pp. 1-21, AGU, Washington, DC.

Roble, R. G., and E. C. Ridley (1994), A thermosphere-ionosphere-mesosphere-electrodynamics general circulation model (TIME-GCM): Equinox solar cycle minimum simulations (30-500 km), *Geophys. Res. Lett., 21*, 417-420, doi:10.1029/93GL03391.

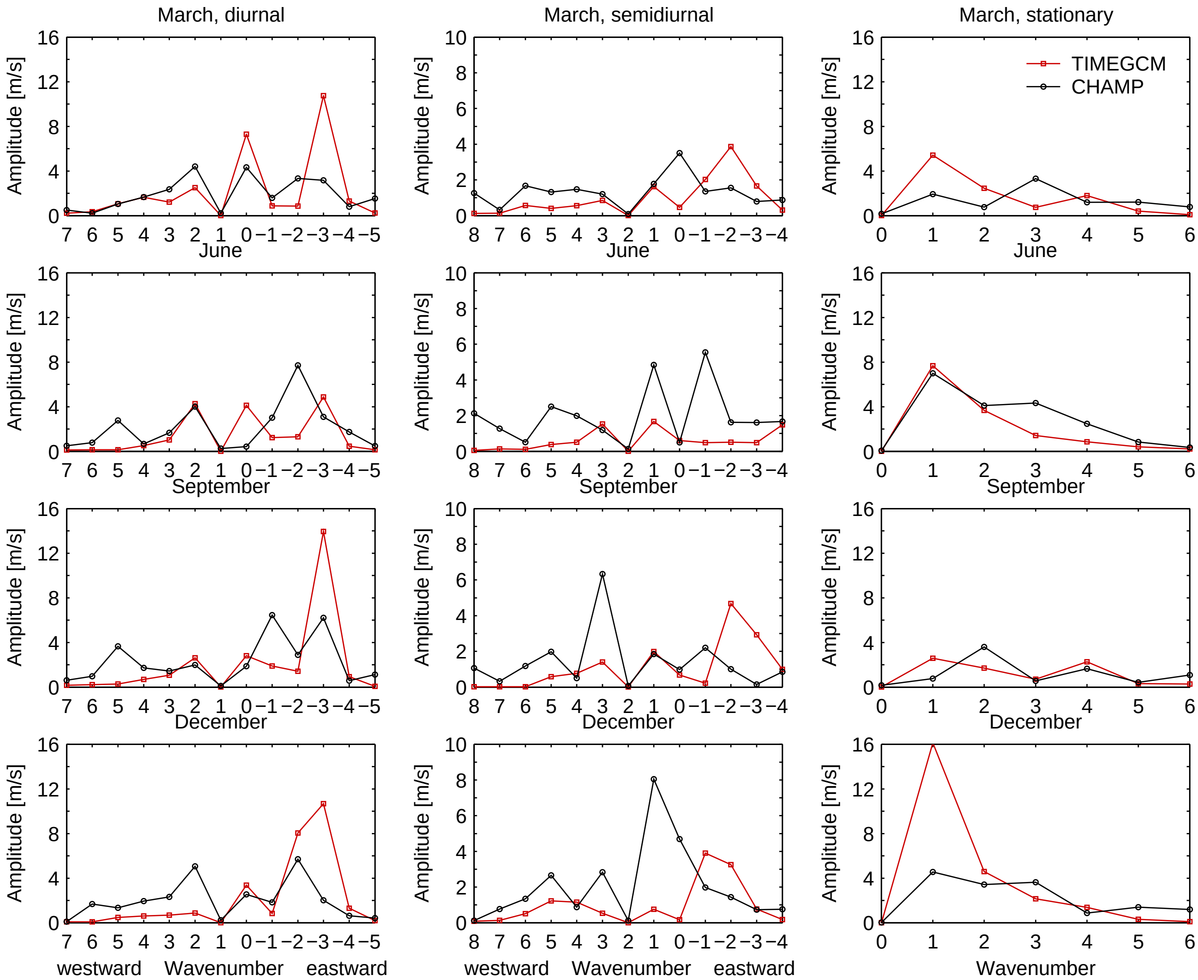

Figure 1. Tidal spectra for TIME-GCM (red) and CHAMP (black) zonal winds from top to bottom for the month of March, June, September, and December, respectively, for diurnal (left panels), semidiurnal (middle panels), and for the stationary contributions (right panels).

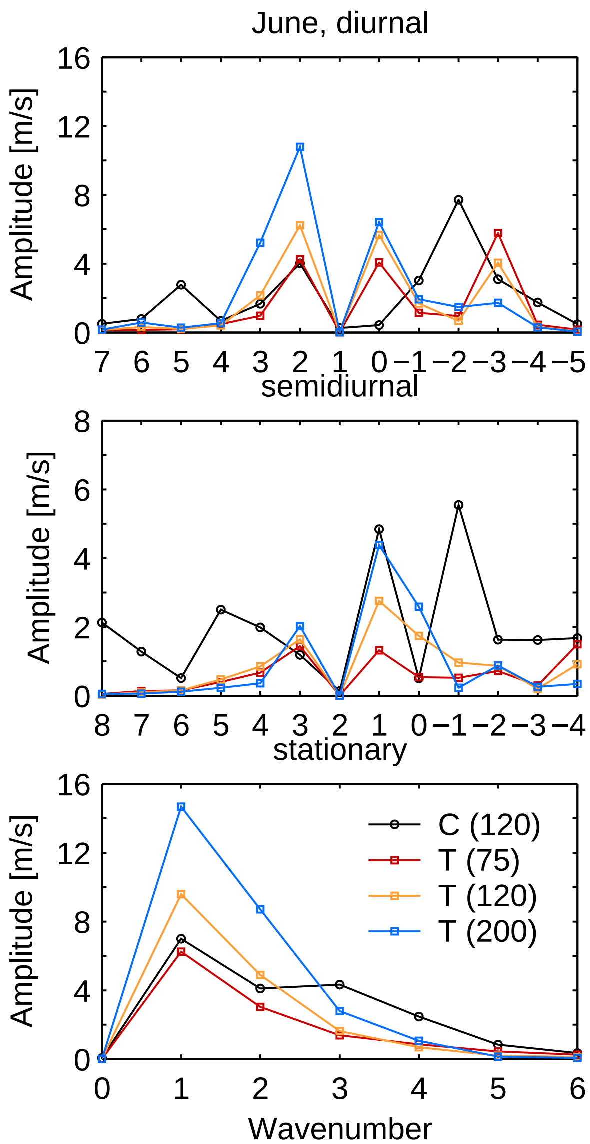

Figure 2. TIME-GCM June tidal spectra for three different solar flux levels (F10.7 = 75, red; F10.7 = 120, orange; F10.7 = 200, blue) for diurnal (top), semidiurnal (middle), and stationary contributions (bottom). Displayed in black are the tidal spectra for CHAMP with an average of F10.7 = 120 for the months of June from 2002-2005.

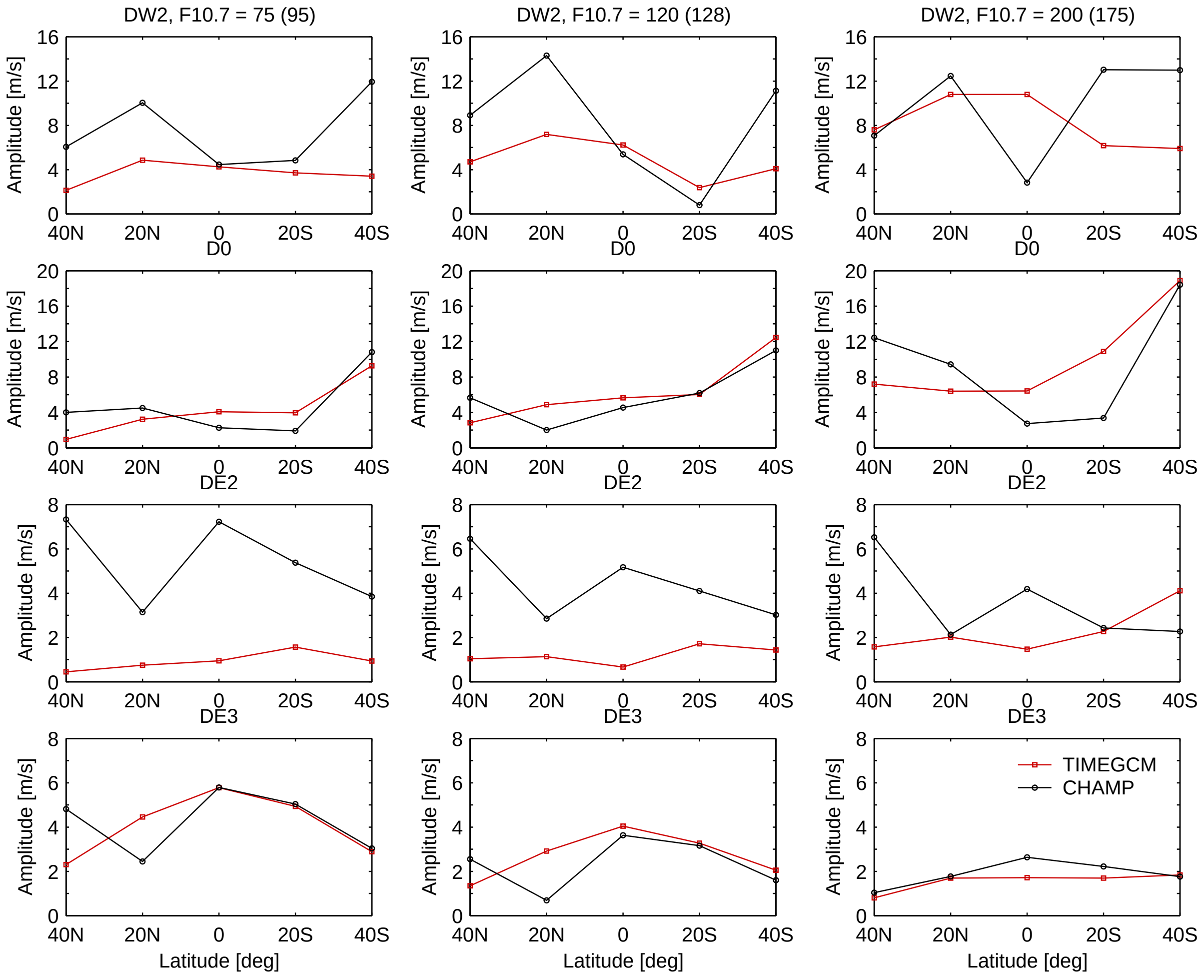

Figure 3. Latitudinal behavior from top to bottom for TIME-GCM (CHAMP) DW2, D0, DE2, and DE3, respectively, from left to right for F10.7 = 75 (95), F10.7 = 120 (128), and F10.7 = 200 (175).